Supporting Information for

Drug-delivery and biological activity in colorectal cancer of a supramolecular porous material assembled from heptameric chromium-copper-adenine entities

*Sandra Mena-Gutiérrez,[a] Ekain Maiza-Razkin,[a] Jon Pascual-Colino,[a,b] Marcos J. Araúzo-Bravo,[c,d,e] Garikoitz Beobide,[a,b] Oscar Castillo,[*a,b] Ainara Castellanos-Rubio,[c,f,g] Daniela Gerovska,[d] Antonio Luque,[*a,b] Sonia Pérez-Yáñez.[a,b]*

Corresponding authors e-mail: oscar.castillo@ehu.eus, antonio.luque@ehu.eus

[a.]Departamento de Química Orgánica e Inorgánica, Facultad de Ciencia y Tecnología, Universidad del País Vasco/Euskal Herriko Unibertsitatea, UPV/EHU, Apartado 644, E-48080 Bilbao, Spain.

[b.]BCMaterials, Basque Center for Materials, Applications and Nanostructures, UPV/EHU Science Park, E-48940 Leioa, Spain

[c.]IKERBASQUE, Basque Foundation for Science; E-48011, Bilbao, Spain.

[d.]Computational Biology and Systems Biomedicine Research Group, Biogipuzkoa Health Research Institute, Donostia, Spain

[e.]Department of Cell Biology and Histology, Faculty of Medicine and Nursing, University of Basque Country (UPV/EHU), Spain

[f.]Biobizkaia Research Institute, E-480903 Barakaldo, Bizkaia, Spain.

[g]Departamento de Bioquímica y Biología Molecular, UPV-EHU, E-48940 Leioa, Bizkaia, Spain.

S1. POWDER X-RAY DIFFRACTION

Powder X-ray diffraction patterns were collected on different conditions upon **Cu6Cr** sample. The image below shows that the release of the crystallization water molecules upon removal from the mother liquid reduces the crystallinity of the sample and implies the displacement of the diffraction peaks to higher angles, indicating the contraction of the volume of the unit cell. To ensure their purity powder X-ray diffraction was performed over samples introduced in a Lindemann capillary and immersed in the synthesis mother liquid. A Rigaku Smartlab automatic diffractometer with a capillary fixation head was used and the diffraction data were collected in continuous rotation in the range $5° < 2\theta < 65°$. The change in crystallinity after dehydration was confirmed by activating a sample by heating it at 30 °C, under vacuum, for four hours. The diffractogram of the activated sample indicates that a high loss of crystallinity occurs. When the activated sample is stored in a humidifier with a degree of humidity of *ca*. 90%, after 24 hours, its weight increases, it recovers crystallinity and its diffractogram is coincident with that of the initial hydrated compound.

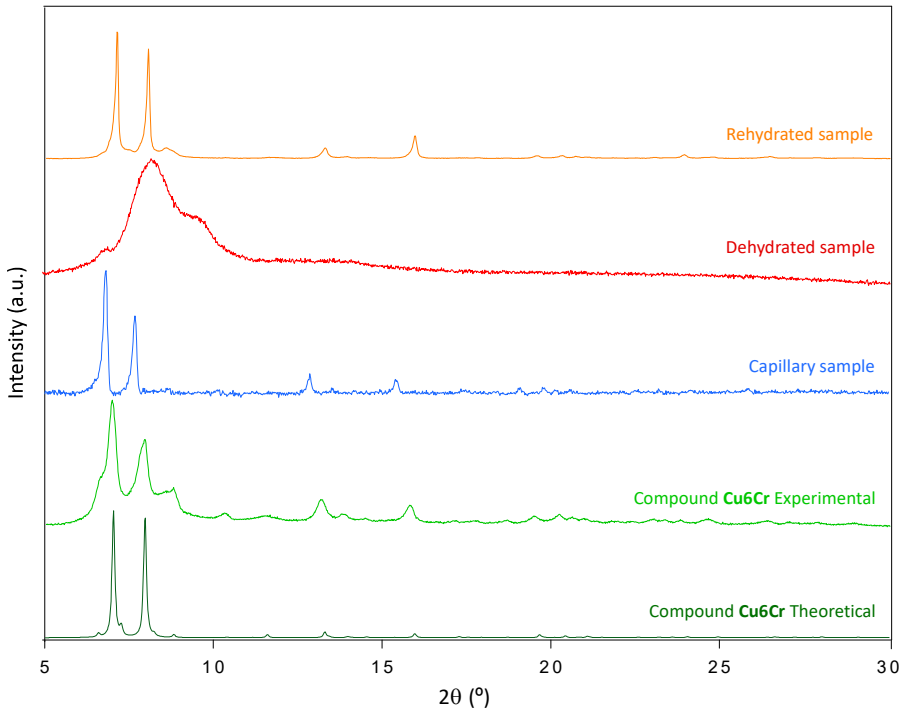

Fig S1. Diffractograms of **Cu6Cr** compound: simulated from the crystal structure (compound **Cu6Cr** theoretical), as obtained after filtration (compound **Cu6Cr** experimental), measured while in a capillary filled with the mother liquid (capillary sample), fully dehydrated sample (30 °C under vacuum for 4 h), and rehydrated sample (stored in a humidifier at RH = 90% for 24 h).

S2. POROSITY OF THE COMPOUND

All the data of the crystal structure (atoms distance/angles and hydrogen bond distances) are described in a previous paper published by our group. (R. Pérez-Aguirre, B. Artetxe, G. Beobide, O. Castillo, I. de Pedro, A. Luque, S. Pérez-Yáñez and S. Wuttke, *Cell Reports Phys. Sci.*, 2021, **2**, 100421).

To assess the suitability of **Cu6Cr** as dock for selected drugs, we have analyzed its main pore features using the crystallographic data (Table S1). Geometric pore size distribution (PSD) was computed by means of a Monte Carlo procedure implemented within a code developed by L. Sarkisov, in which the Lennard-Jones (LJ) universal force field parameters are used to describe the SMOF atoms while the accessible pore volume is assessed by a gradually increasing probe size (L. Sarkisov, R. Bueno, M. Sutharson and D. Fairen, Materials Informatics with PoreBlazer v4.0 and the CSD MOF Database. *Chem. Mater.*, 2020, **32**, 9849–9867). The results are shown in Fig S2.

Table S1. Porosity data for all reported compounds.

Compound	d_{Pore} (mode, Å)		Void volume (Å^3)	Void (%)	Surface area (m^2/g)	Pore volume (cm^3/g)
	Min	max				
Cu_6Cr	4.6	6.3	4530	49	840	0.428

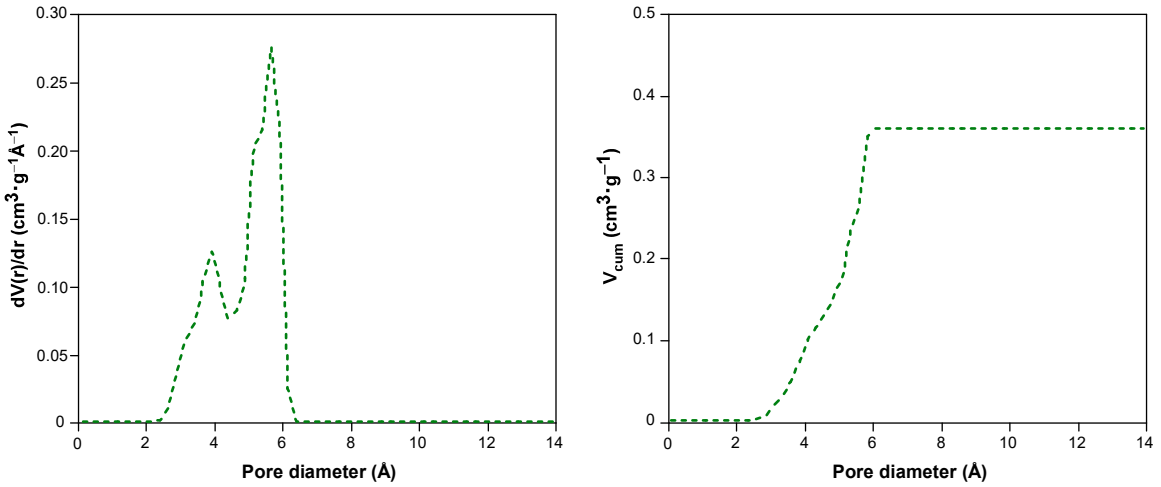

(a) (b)

Fig S2. (a) Derivative representation of the geometric pore volume of compounds. (b) Cumulative representation of the geometric pore volume of compound **Cu6Cr**.

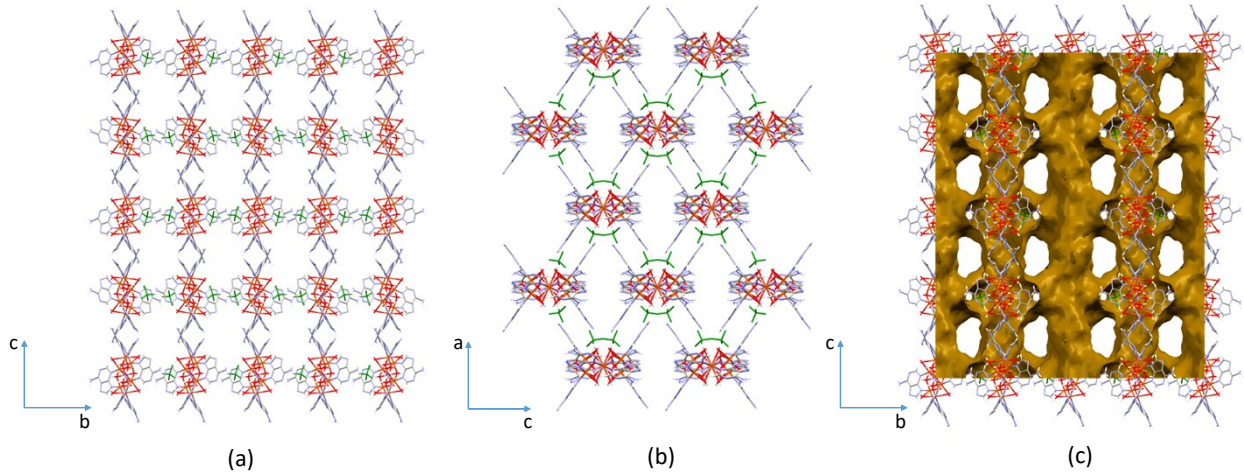

Fig S3. Channels for compound **Cu6Cr** with the sulphate anion in green along the crystallographic (a) *a* axis and (b) *b* axis. (c) Representation of the channels contact surface in the porous structure in brown.

S3. SORPTION DATA QUANTIFICATION BY PROTON NUCLEAR MAGNETIC RESONANCE (^{1}H-NMR)

^{1}H-NMR spectra of analyzed samples were acquired on a Bruker AVANCE 5OO spectrometer (one-bay; 500 MHz) at 293 K. For that purpose, the adsorption experiment was repeated but using deuterated water (D_2O): 50 mg of compound **Cu6Cr**, 2 mL of deuterated water and 50 mg of the calibration standard (benzyl alcohol**,** isopropanol and glucose) in each case. The samples were kept under continuous agitation for 24 hours at 30 °C). Later, the suspension is centrifuged to separate the solid from the solution and to 1 mL of the liquid phase 100 µL of a 5% *t*-butanol (internal standard) heavy water solution were added. The same procedure was applied for each adsorptive but without the addition of the porous material (**Cu6Cr**) in order to determine the initial adsorptive amount in the adsorption experiment. ^{1}H-NMR measurement was performed on the centrifuged solution and the characteristic signals of the adsorptive and *t*-butanol were used to quantify the amount of the adsorptive remaining in solution by difference with the initial value to determine the amount adsorbed within the porous material. The following figures illustrate the blank and post-sorption experiment solution ^{1}H-NMR spectra, indicating the signals employed for the quantification.

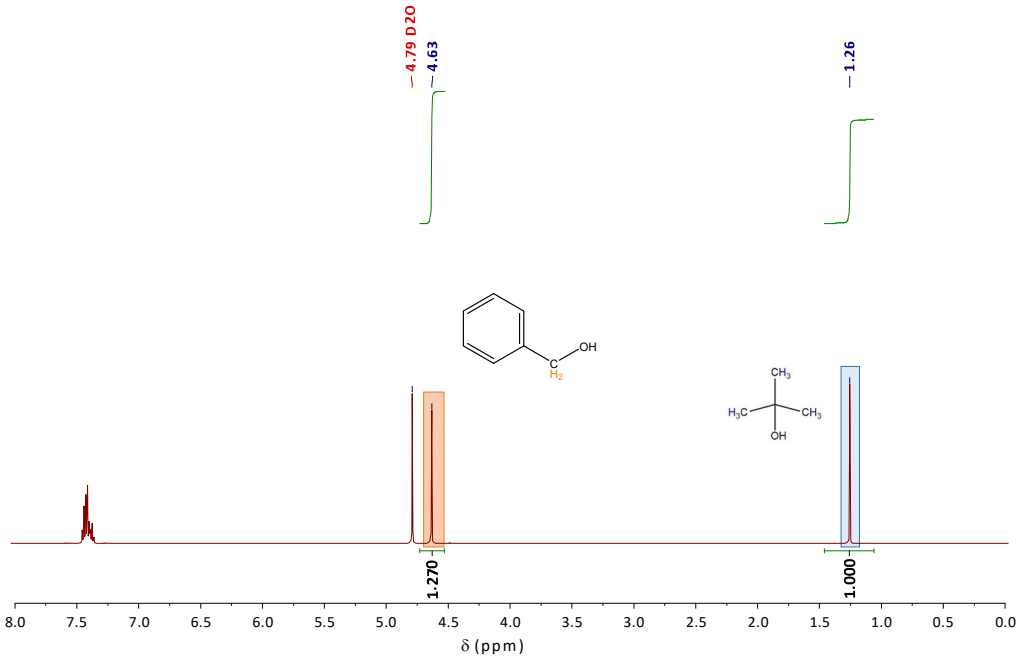

(a)

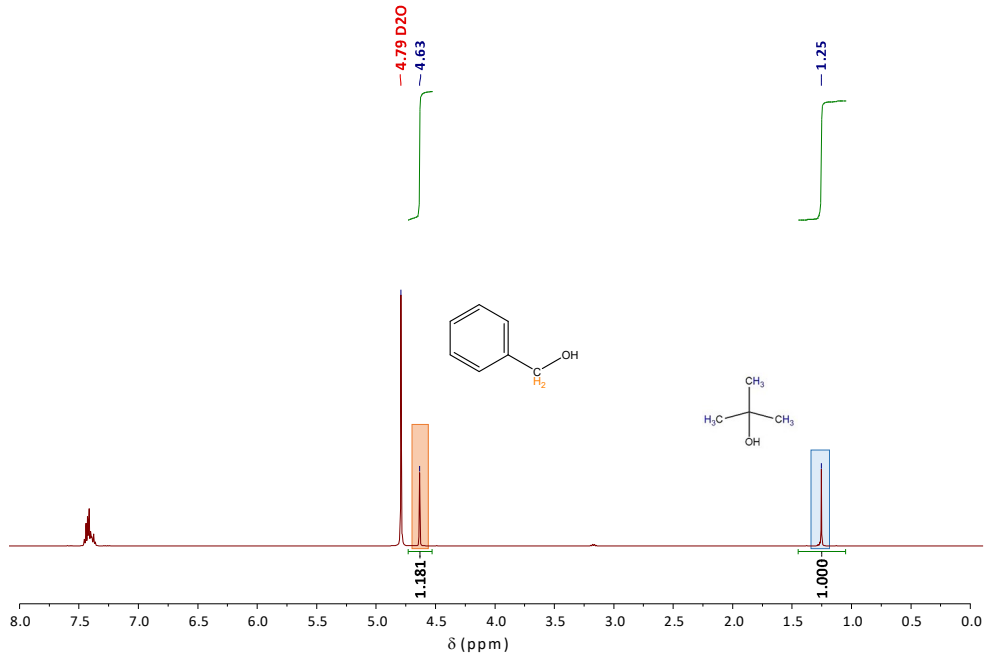

(b)

Fig S4. ^{1}H-NMR spectra for blank (upper) and experimental (bottom) samples of compound **Cu6Cr** with benzyl alcohol.

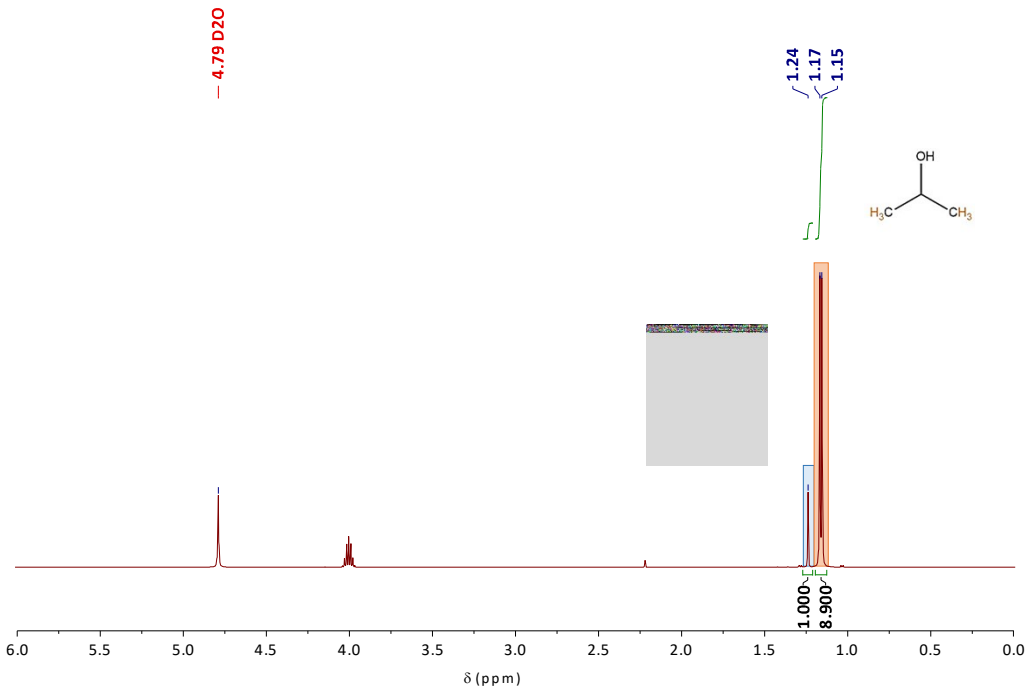

(a)

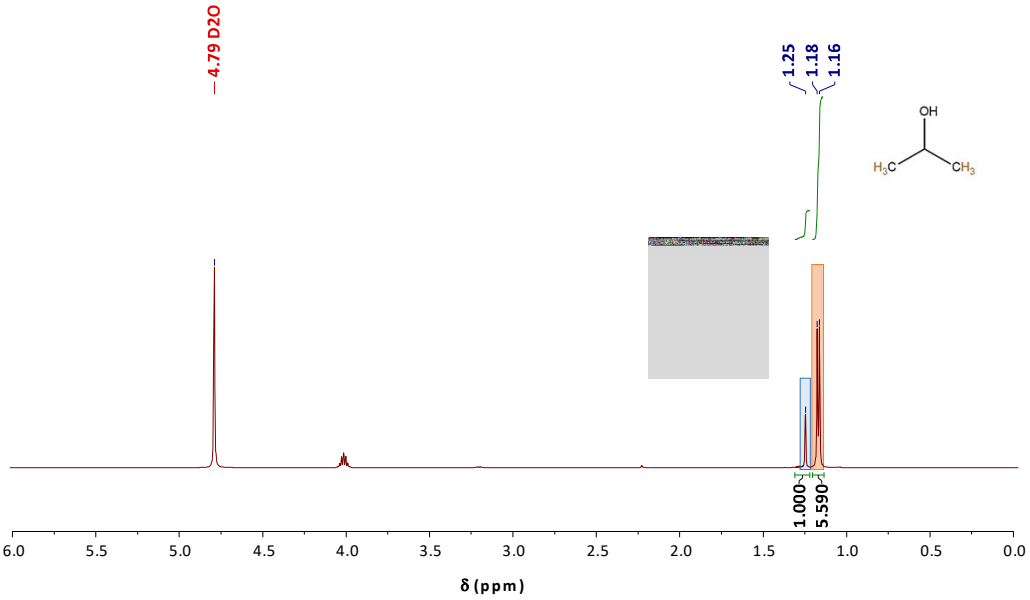

(b)

Fig S5. ^{1}H-NMR spectra for blank (upper) and experimental (bottom) samples of compound **Cu6Cr** with isopropanol.

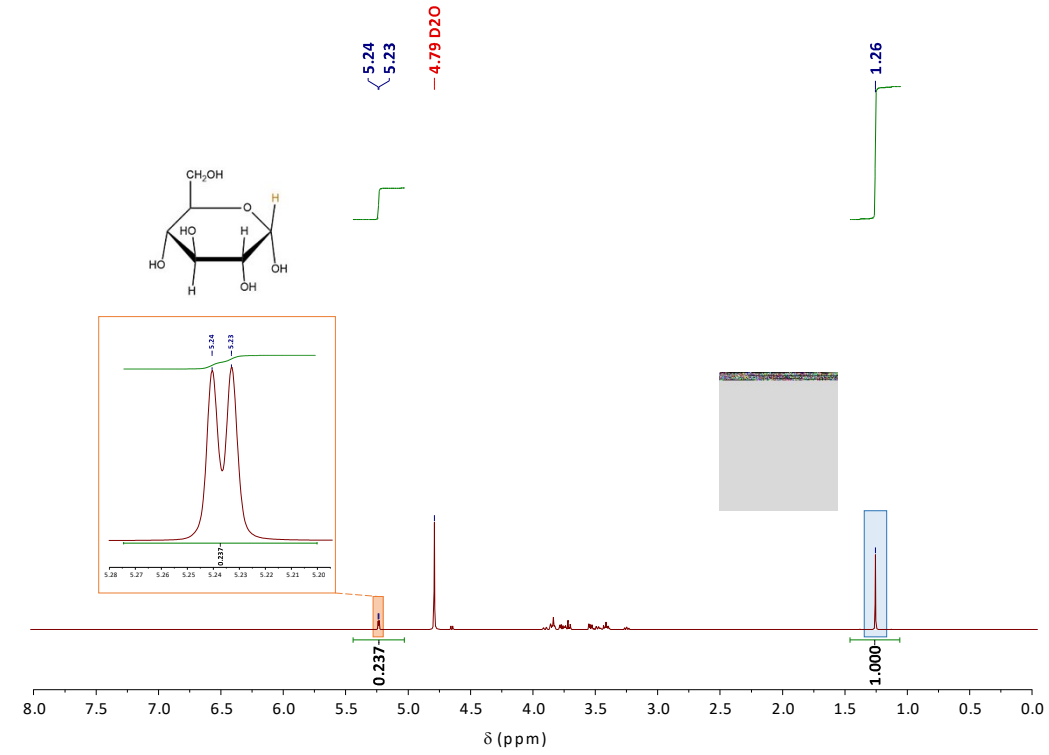

(a)

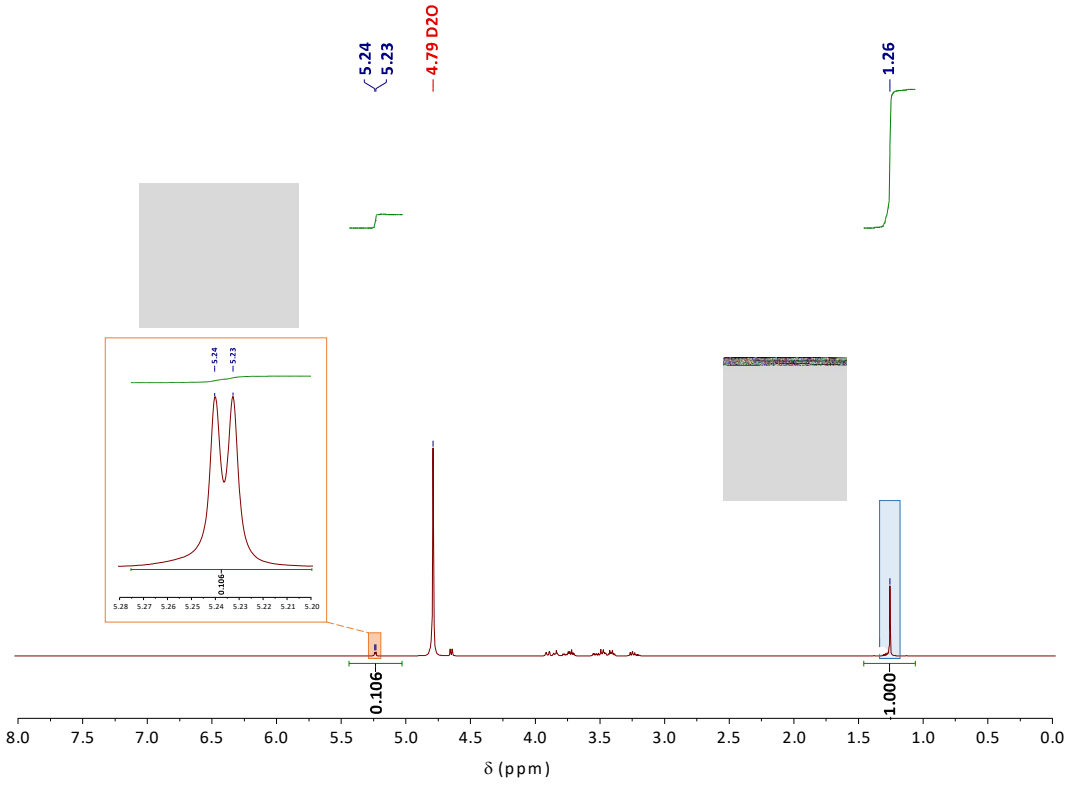

(b)

Fig S6. ^{1}H-NMR spectra for blank (upper) and experimental (bottom) samples of compound **Cu6Cr** with glucose.

S4. FTIR SPECTRA AND POWDER X-RAY DIFFRACTION PATTERNS OF THE DRUG LOADED COMPOUND Cu6Cr

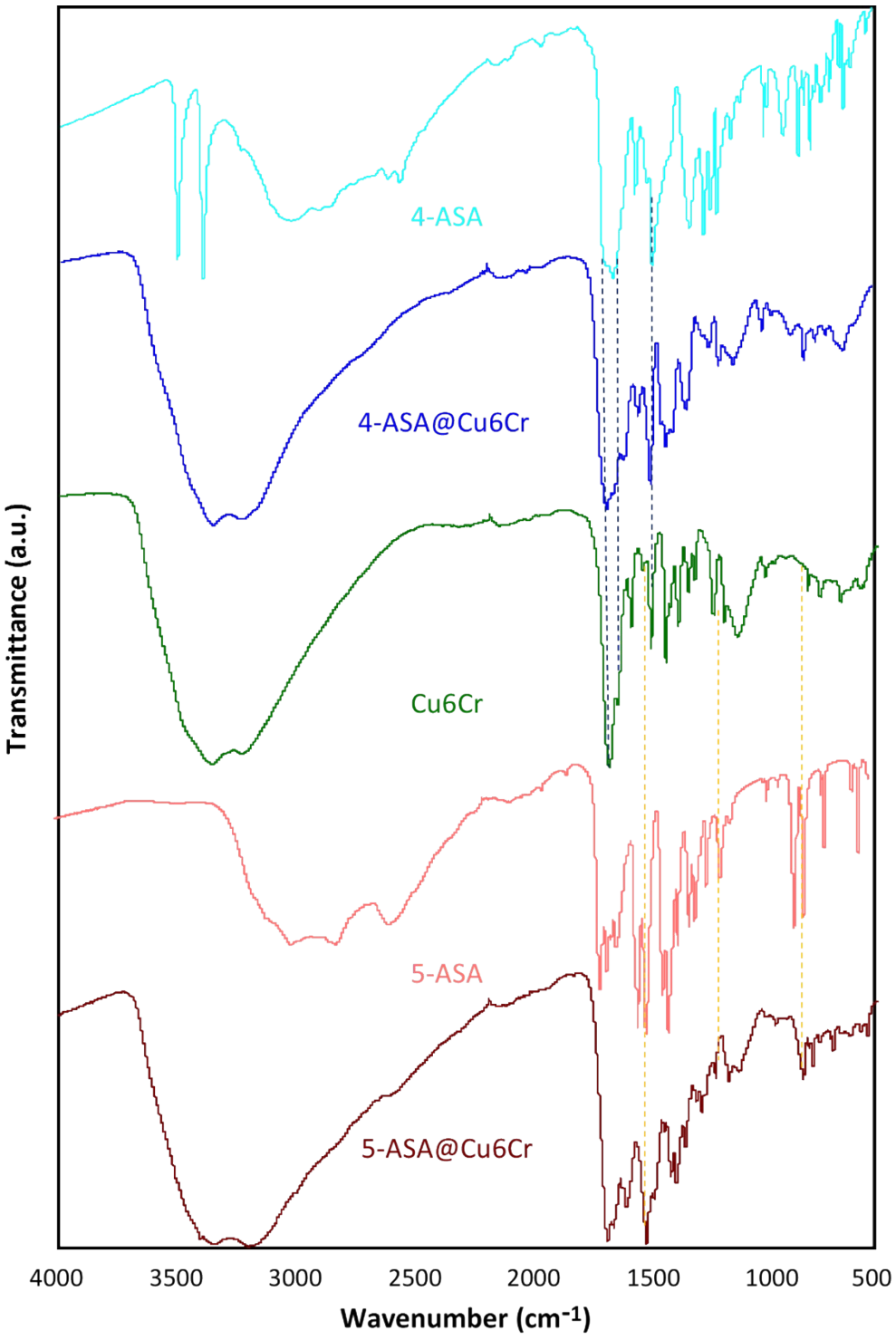

Fig S7. FTIR of compound **Cu6Cr** after being loaded with 5-aminosalicylic acid (**5-ASA@Cu6Cr**) and 4-aminosalicylic acid (**4-ASA@Cu6Cr**).

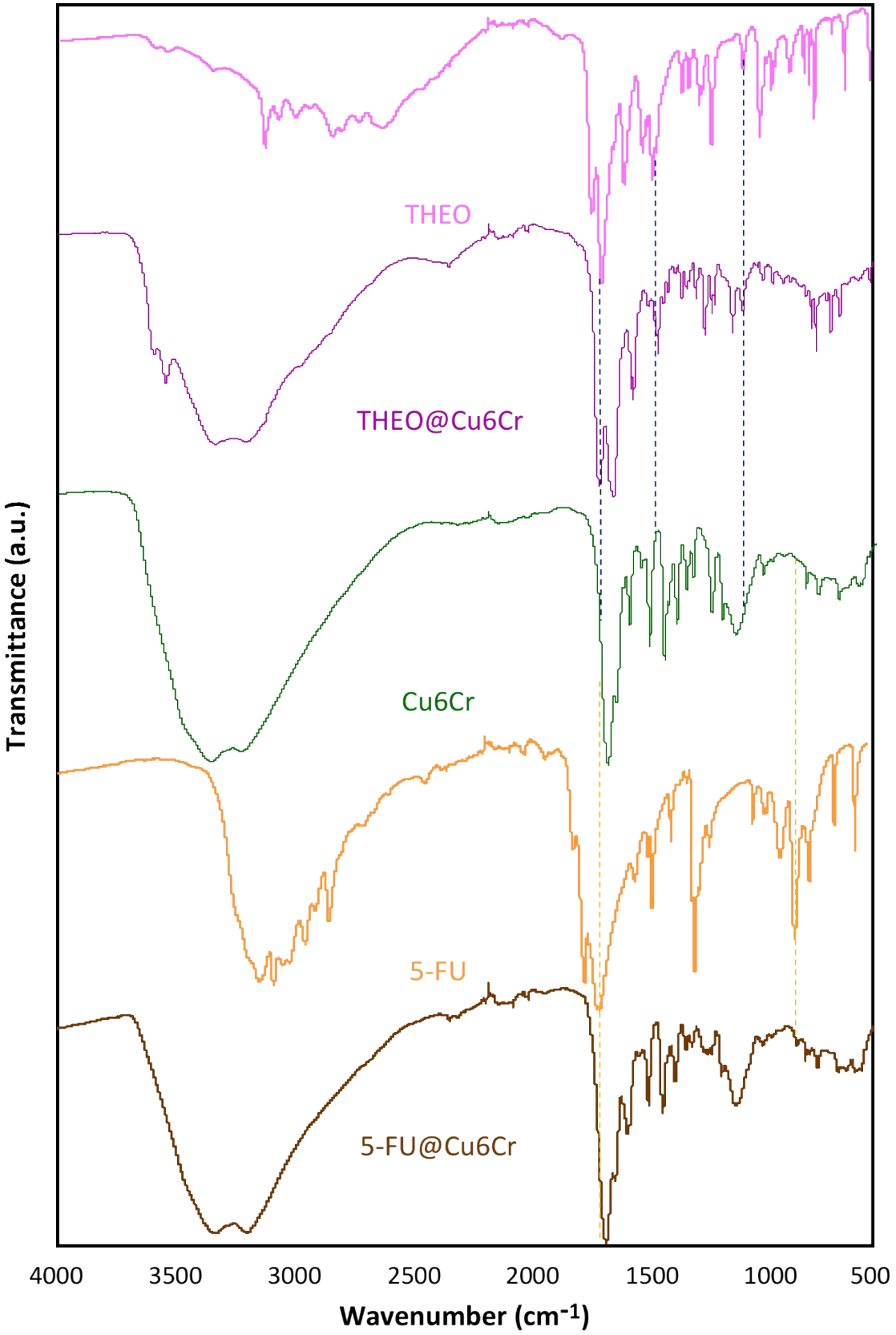

Fig S8. FTIR of compound **Cu6Cr** after being loaded with 5-fluorouracil (**5-FU@Cu6Cr**) and theophylline (**THEO@Cu6Cr**).

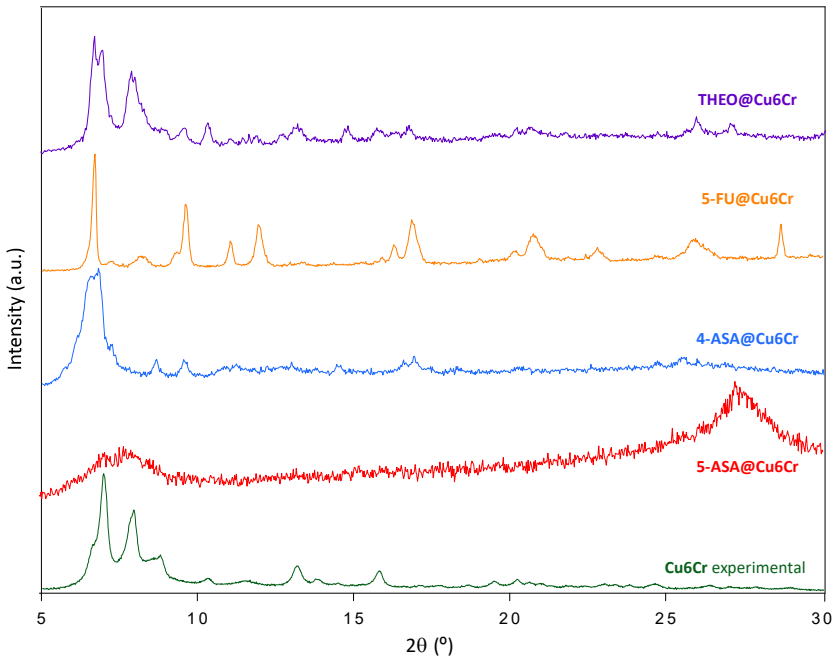

Fig S9. Powder diffraction patterns of compound as-prepared **Cu6Cr and** loaded with 4-aminosalicylic acid (**4-ASA@Cu6Cr**), 5-aminosalicylic acid (**5-ASA@Cu6Cr**), 5-fluorouracil (**5-FU@Cu6Cr**) and theophylline (**THEO@Cu6Cr**).

S5. ADSORPTIVE VOLUMEN AND SHAPE

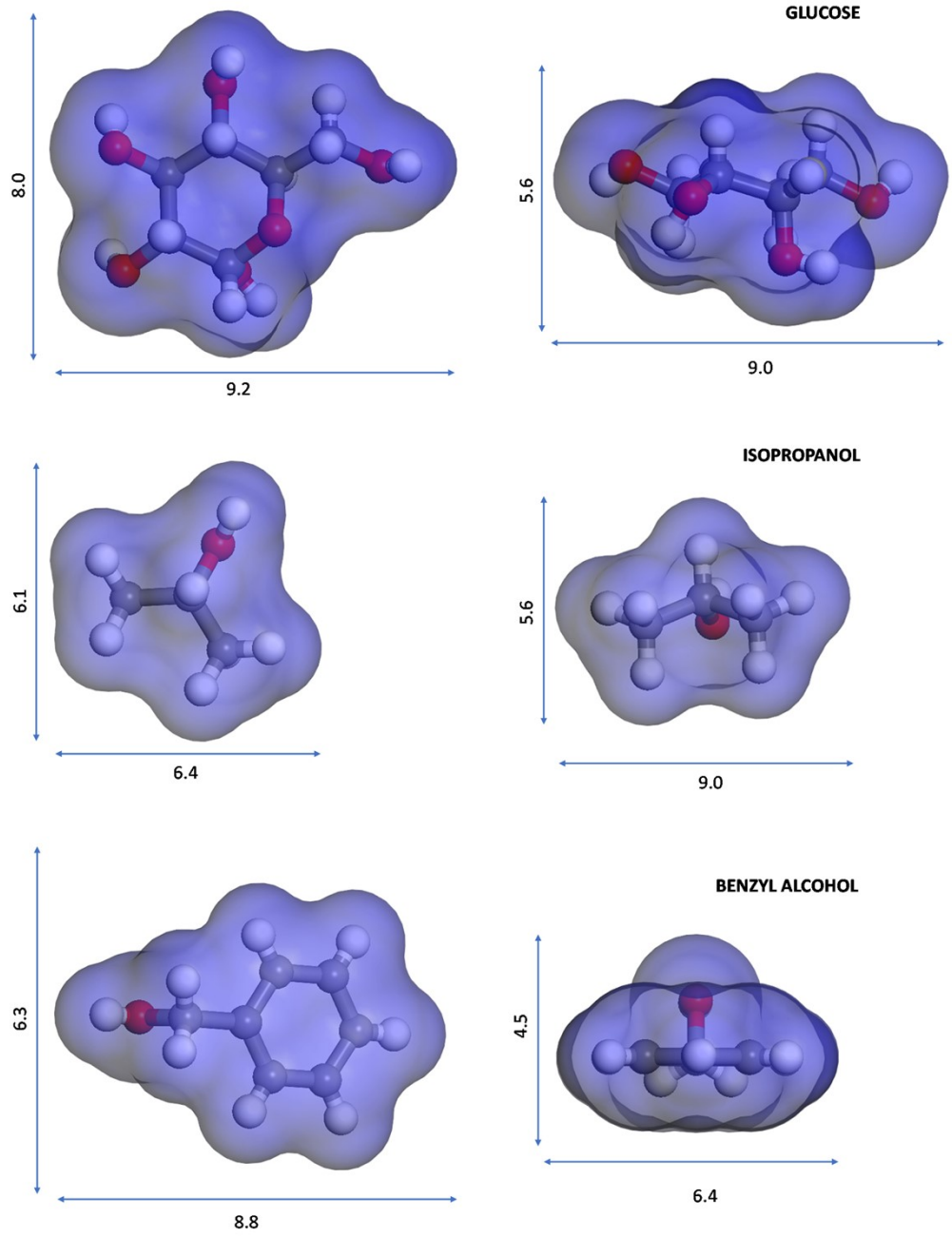

Fig S10. Shape and dimensions (Å) of the adsorptive molecules used as calibration standards for the magnetic sustentation technique. The same scale has been used for all the images to facilitate a direct visual comparison between them. A 1.0 Å probe has been employed to define the Connolly surface of the adsorptive molecules (Materials Studio, *BIOVIA Materials Studio*: 2017 R2, 17.2.0.1626, package).

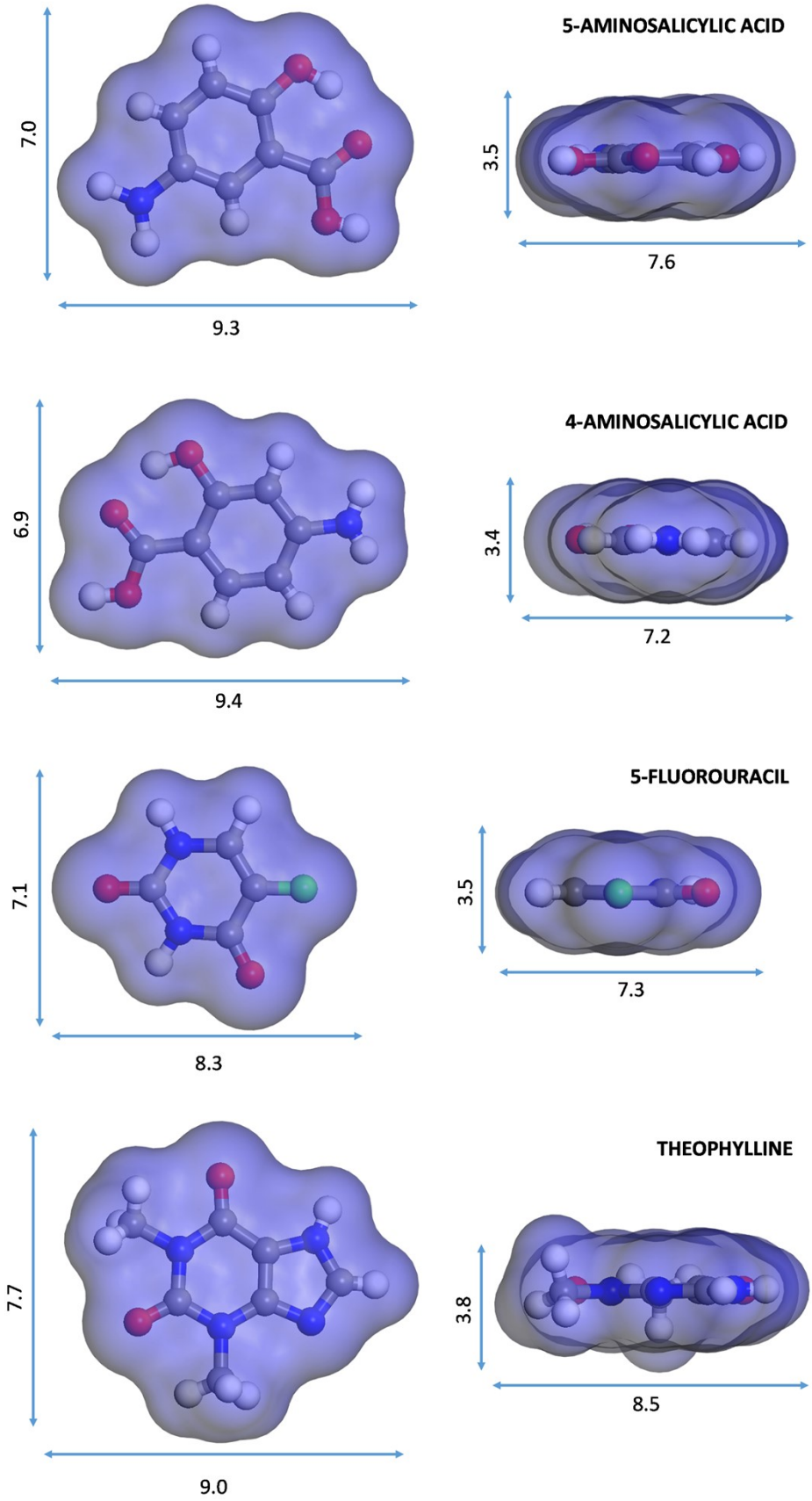

Fig S11. Shape and dimensions (Å) of the drug molecules.

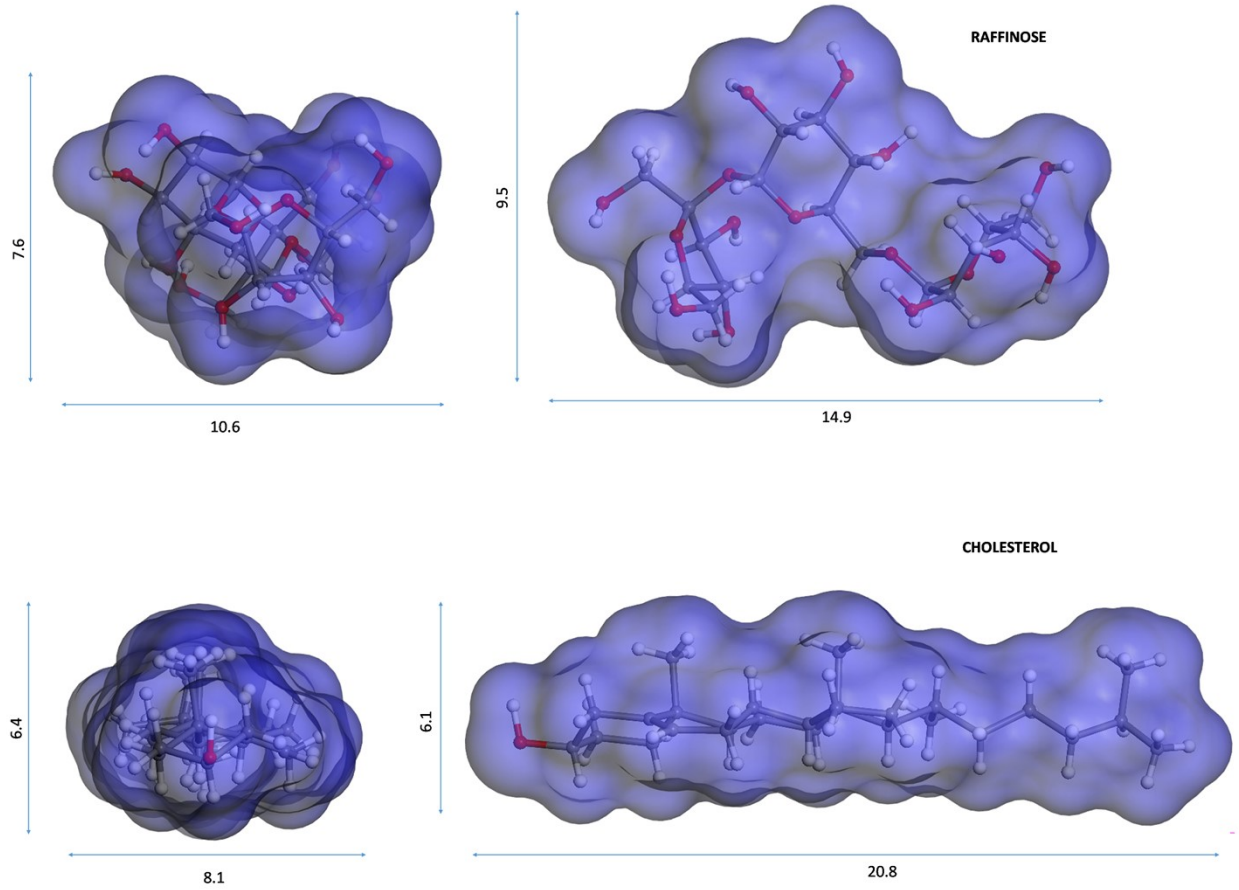

Fig S12. Shape and dimensions (Å) of the release controlled molecules.

S6. RNA-SEQ TRANSCRIPTOMIC ANALYSIS

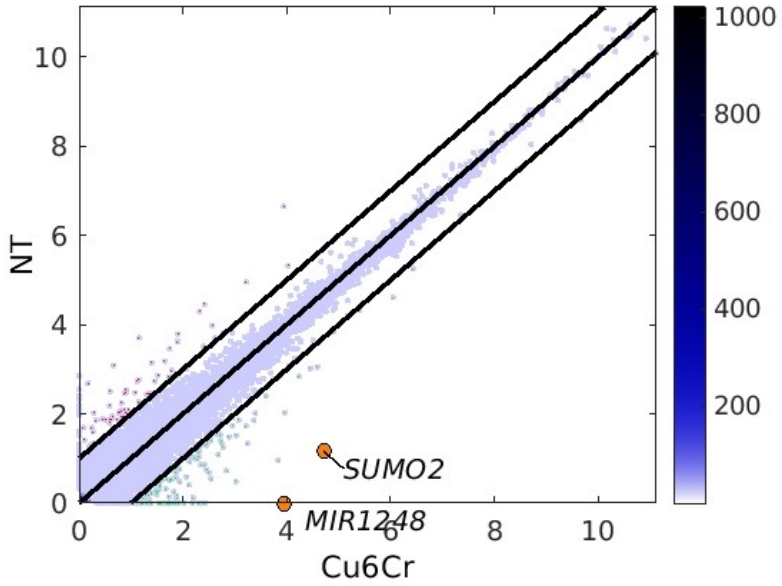

Figure S13. Pairwise scatter plot **Cu6Cr** vs NT (non-treated).

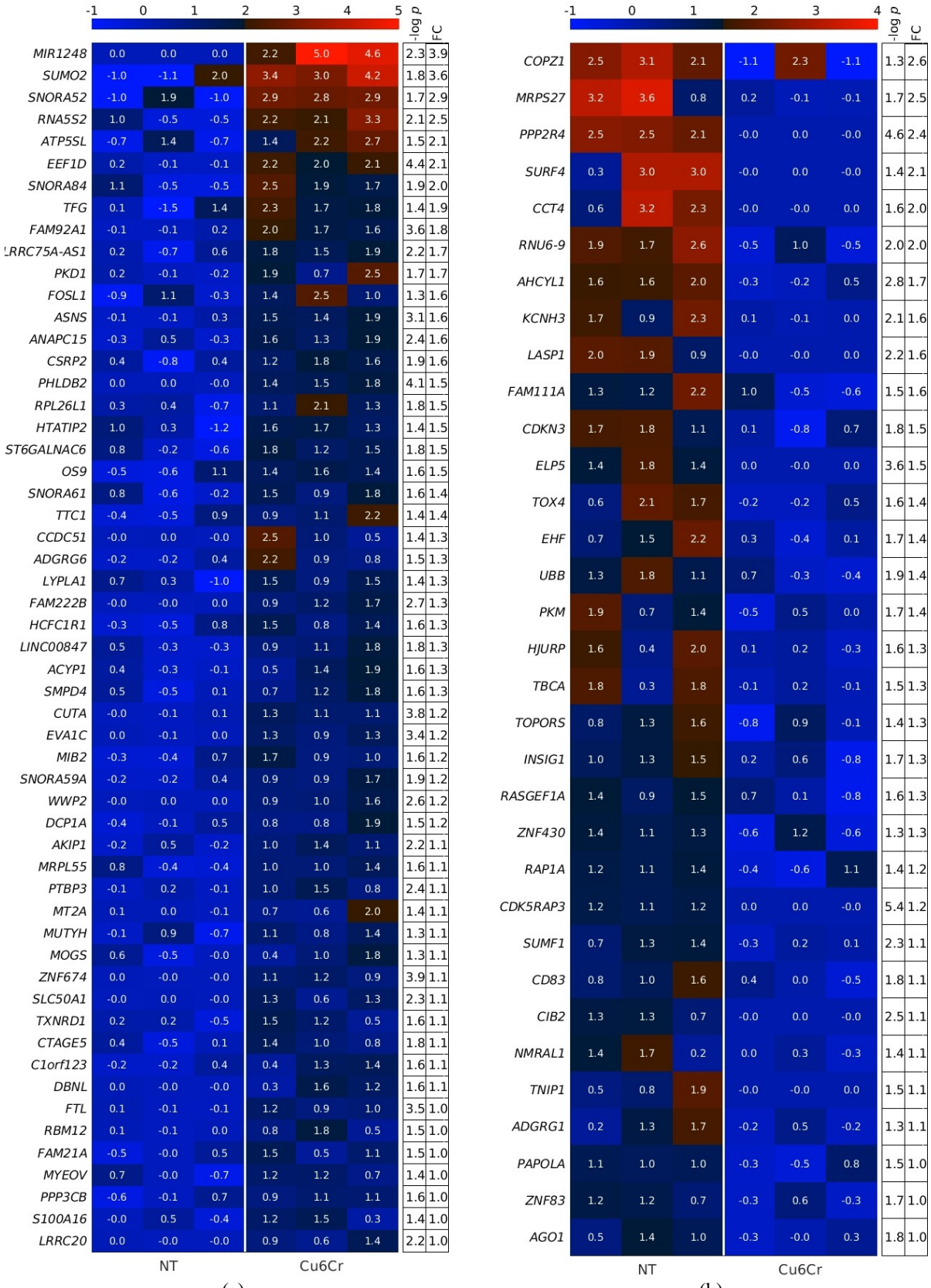

Fig S14. Heat map. **Cu6Cr**-NT-Log_2(2): (a) up-expressed transcripts and (b) down-expressed transcripts.

S7. DESORPTION KINETIC FITTING

Table S2. Release kinetics fitting parameters for different kinetic models.

	First order model[a]		Higuchi model[b]		Korsmeyer-Peppas model[c]		
	$K\ (h^{-1})$	R^2	$K_H\ (mg{\cdot}g^{-1}{\cdot}h^{-1/2})$	R^2	K_K	n	R^2
4-ASA	0.235	0.9912	125.56	0.9896	0.222	0.720	0.9736
5-ASA	0.147	0.9958	101.14	0.9889	0.170	0.746	0.9880
5-FU	0.166	0.9942	86.68	0.9971	0.203	0.562	0.9789
THEO	0.319	0.9926	100.90	0.9905	0.202	0.659	0.8956
RAFF@5-FU	0.133	0.9948	74.71	0.9939	0.152	0.663	0.9859
CHOL@5-FU	0.096	0.9936	68.42	0.9509	0.033	1.323	0.9378

[a] Fitting data corresponding to the first 4 h of the desorption process.

[b] T. Higuchi, *J. Pharm. Sci.*, 1963, **84**, 1464. Fitting data corresponding to the first 10 h of the desorption process

[c] R. W. Korsmeyer, R. Gurny, E. Doelker, P. Buri, N. A. Peppas, *Int. J. Pharm.*, 1983, **15**, 25. Fitting data corresponding to the first 10 h of the desorption process.

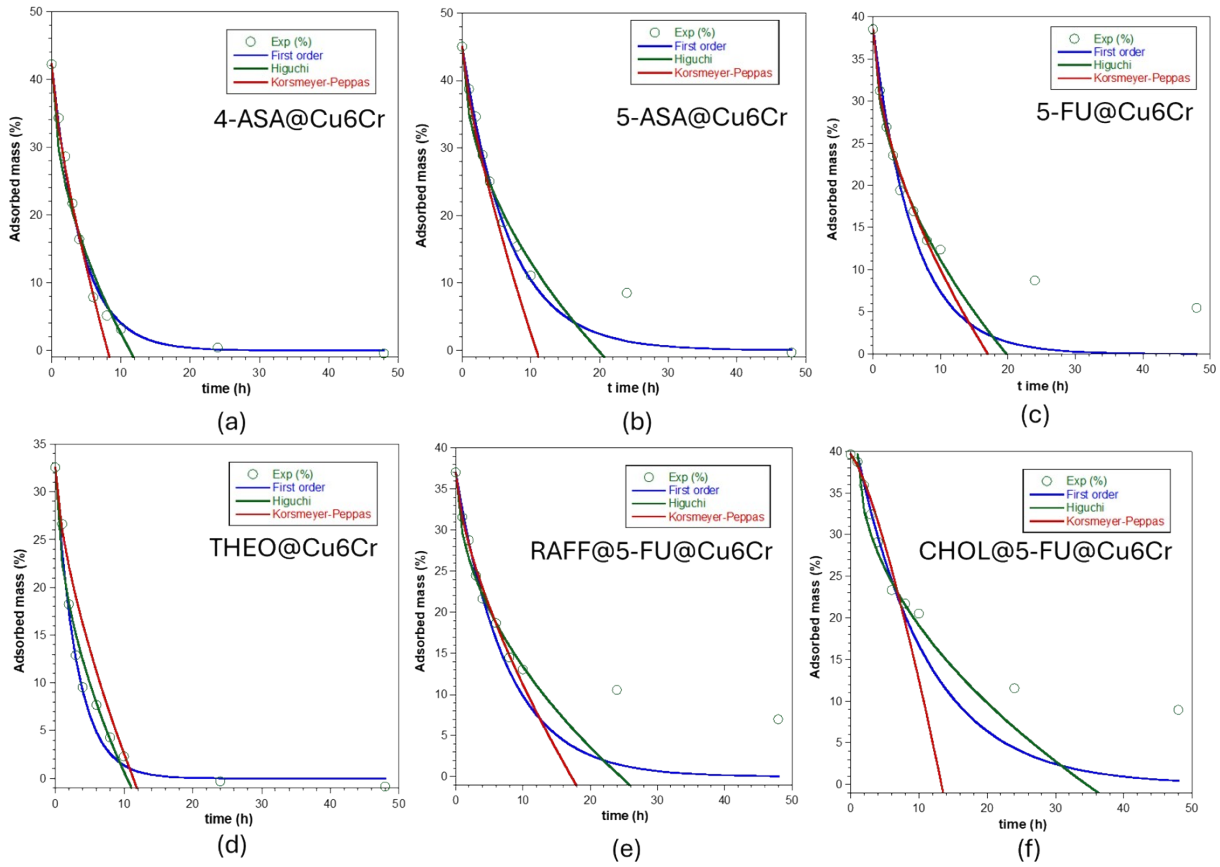

Fig S15. Drug desorption isotherms in aqueous solution for **Cu6Cr** showing the best fitting curves for the first order, Higuchi and Korsmeyer-Peppas models.